Chapter 18
Fatigue of Joints

18.1 Introduction
18.2 Lugs
18.3 Symmetric butt joints with rows of bolts or rivets
18.4 Bolts loaded in tension
18.5 Riveted and bolted joints with eccentricities
18.6 Adhesive-bonded joints
18.7 General discussion on predictions of fatigue properties of joints
18.8 Major topics of the present chapter
References

. . . fatigue is the art of joints . . .

18.1 Introduction

Fatigue failures in structures frequently occur in joints. Various catastrophic accidents due to fatigue have been reported in the literature. As a consequence joints are a major issue for designing against fatigue. The prime purpose of a joint is to transmit loads from one element of the structure to an other element. The variety of different joint configurations is very large. Some elementary types of joints are shown in Figure 18.1.

A significant difference between two categories of joints is associated with the question whether it should be possible to disassemble and reassemble a joint, or whether that is not necessary. The lug type joint and the bolted joint are in the first category. However, riveted lap joints, bonded lap joints and welded joint, including spot welded joints, are supposed to remain in the as-produced condition. Another noteworthy aspect of joints is associated with eccentricities in the joint. The bolted joint in Figure 18.1 is fully symmetric with respect to the line of the applied load. But that is not true for the two non-symmetric lap joints in Figure 18.1. As a result of the eccentricity in these joint, bending is introduced by the applied tensile

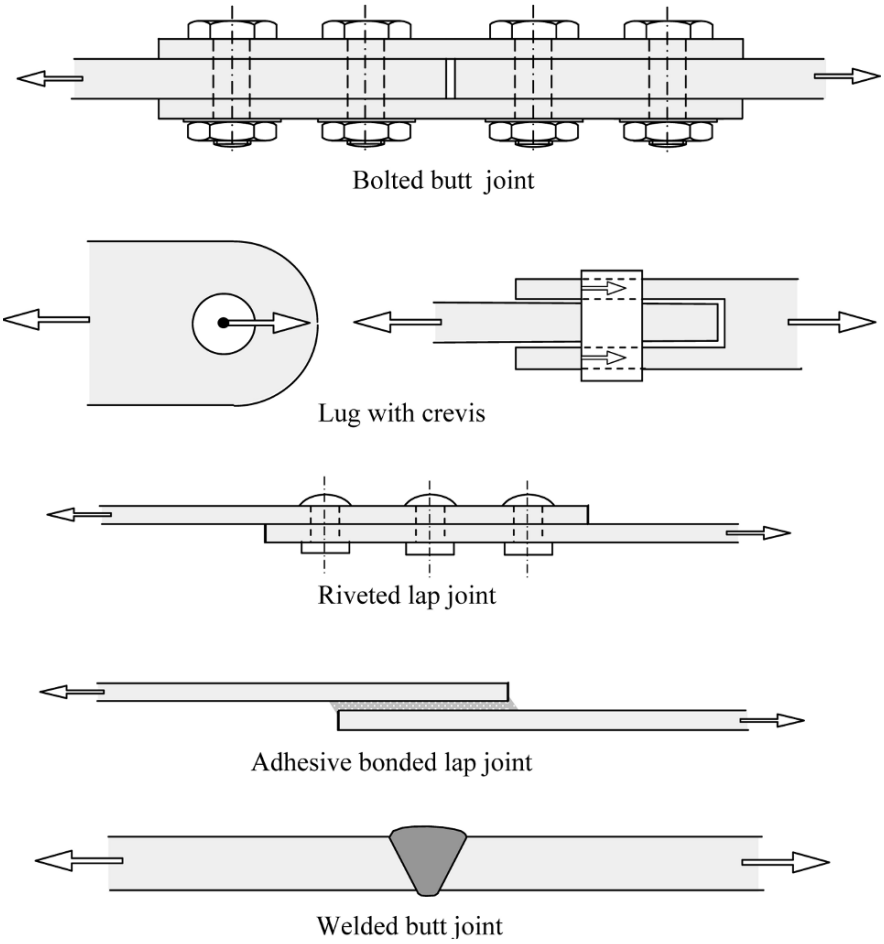

Fig. 18.1 Symmetric butt joints and lap joints with eccentricities.

load. The additional bending, referred to as secondary bending, will increase notch effects in these joints. Furthermore, fasteners in a simple lap joints are loaded in single shear whereas bolts in the symmetric joint are loaded in double shear which appears to be a more favorable situation. Still another complexity is the occurrence of fretting in lugs and bolted and riveted joints. Once again, the variety of joints is just large. Moreover, the number of design parameters for each type of joint also contributes to a broad spectrum of design questions. Variables included are associated with joint dimensions, production variables and selected materials.

In view of the above diversity, several types of joints are discussed in separate sections. Fatigue of lugs is covered in Section 18.2. A lug is the most simple and elementary joint. Symmetric joints with more fasteners loaded in shear are discussed in Section 18.3. Bolts loaded in tension offer different problems dealt with in Section 18.4, including pre-tensioning. Characteristic aspects of riveted joints are associated with the riveting process, fretting corrosion and secondary bending. These aspects are discussed in Section 18.5. Adhesive bonded lap joints as an alternative to riveted lap joints are briefly addressed in Section 18.6. Fatigue of welded joints is covered in a separate chapter (Chapter 19) because characteristic aspects of welded joints are entirely different from problems associated with mechanical joints. Actually, welded joints are supposed to be an integral connection rather than joining different structural elements. Because joints offer specific prediction problems, some general comments are presented in Section 18.7. Major aspects of the present chapter are summarized in Section 18.8

18.2 Fatigue of lugs

The lug connection is an elementary joint with a single pin or bolt as described earlier in Chapter 3, see Figure 3.17. The stress concentration factor (K_t) of a lug is relatively high, see Figure 3.19. Attractive features of a lug connection are: (1) assembling and disassembling is relatively easy, and (2) rotation between the two connected parts is possible which may be necessary in view of specific functions, e.g. in push/pull mechanisms. In cases of statistically indeterminate structures, it may be desirable to have a zero moment at a pin connection which can be accomplished by a small rotation in a lug connection.

Observations on fatigue of lugs were already discussed in Chapter 15 on fretting corrosion. It was shown that the fatigue limit could be very low, see Figures 15.11 and 15.12. The fatigue strength reduction factor, K_f, can be significantly larger than the stress concentration factor K_t. The low fatigue limit is caused by fretting corrosion inside the hole, which initiates microcracks at low stress amplitudes. At higher stress amplitudes with lower endurances, the detrimental effect of fretting corrosion is much less because microcracks are then initiated early in the fatigue life anyway, also if fretting does not occur.

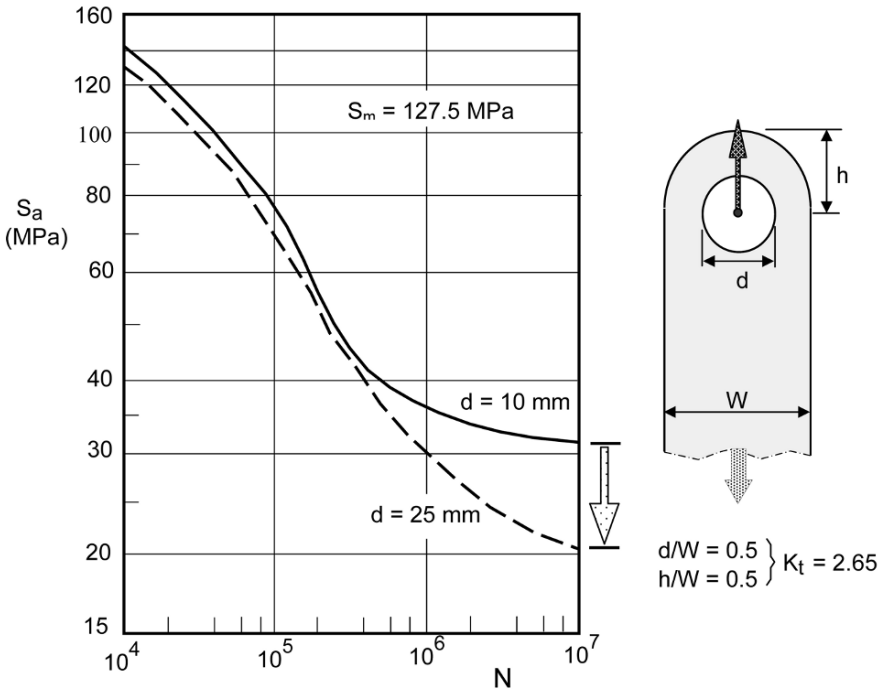

Fig. 18.2 Size effect on the S-N curve of a lug. Material: Al-alloy 2024-T3 [1].

As discussed in Chapter 15, fretting corrosion is depending on the amplitude of the fretting movements, see Figure 15.7. The fretting movement amplitude inside the hole of the lug is larger for a larger lug because the amplitude is proportional to the size of the lug. As a consequence, it should be expected that the fatigue limit of a lug depends on the size of the lug. This has been confirmed by experiments. The results for lugs of an Al-alloy in Figure 18.2 show that the fatigue limit of a large lug is 35% lower than for a small lug although the shapes are similar, and thus the same K_t is applicable. This size effect is much larger than predicted by the size effect equations discussed in Section 7.2 for notches where fretting is not involved. Figure 18.2 also shows that the size effect due to fretting disappears at lower endurances in agreement with the much smaller effect of fretting during low-cycle fatigue.

Larsson [2] has analyzed a large amount of S-N data of lugs of two Al-alloys (2024-T3 and 7075-T6), and later the same was done for Ti-alloys, high-strength steels and Mg-alloys in the aircraft industry [3]. Larsson arrived at an empirical equation to predict the fatigue strength of a lug. A

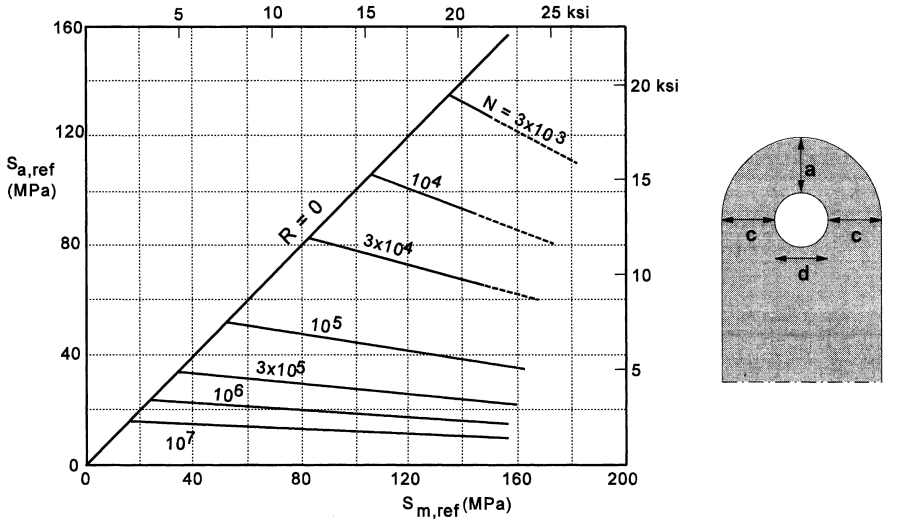

Fig. 18.3 Fatigue diagram for a reference lug with dimensions $a = c = d = 10$ mm (0.4") according to Larsson [2]. Material: Al-alloy 2024-T3.

reference lug was defined by the dimensions $a = c = d = 10$ mm (0.4"), see Figure 18.3. The analysis of many data led to the fatigue diagram for the reference lug, which is presented in Figure 18.3 for the Al-alloy 2024-T3. Larsson derived a second diagram for the Al-alloy 7075-T6. Symbols of the stress amplitude and mean stress for the reference lug are $S_{a,\text{ref}}$ and $S_{m,\text{ref}}$. The fatigue strength for another lug, defined by S_a and S_m, is now obtained by the following equations (stress calculated on the net section):

$$\frac{S_a}{S_{a,\text{ref}}} = \frac{S_m}{S_{m,\text{ref}}} = 1 + \theta(k_1 k_2 - 1)$$

$$\text{with} \quad k_1 = \left(\frac{ad}{c^2}\right)^{0.5}, \quad k_2 = \left(\frac{10}{d}\right)^{0.2} \quad (d \text{ in mm}) \tag{18.1}$$

$$\theta = 0.25 \log N - 0.5 \text{ for } N = 10^3 \text{ to } 10^6 \quad \text{and} \quad \theta = 1 \text{ for } N \geq 10^6$$

As shown in this equation, k_1 accounts for the shape of the lug, k_2 for the size effect, and θ for the decreasing effect of fretting corrosion at lower endurances. It should be emphasized that Larsson's equation is empirical. The equation was obtained by a multi-variable regression analysis of many test data. It gives approximate indications of the fatigue strength. Fatigue data of lugs are also presented in [4]. More accurate information would

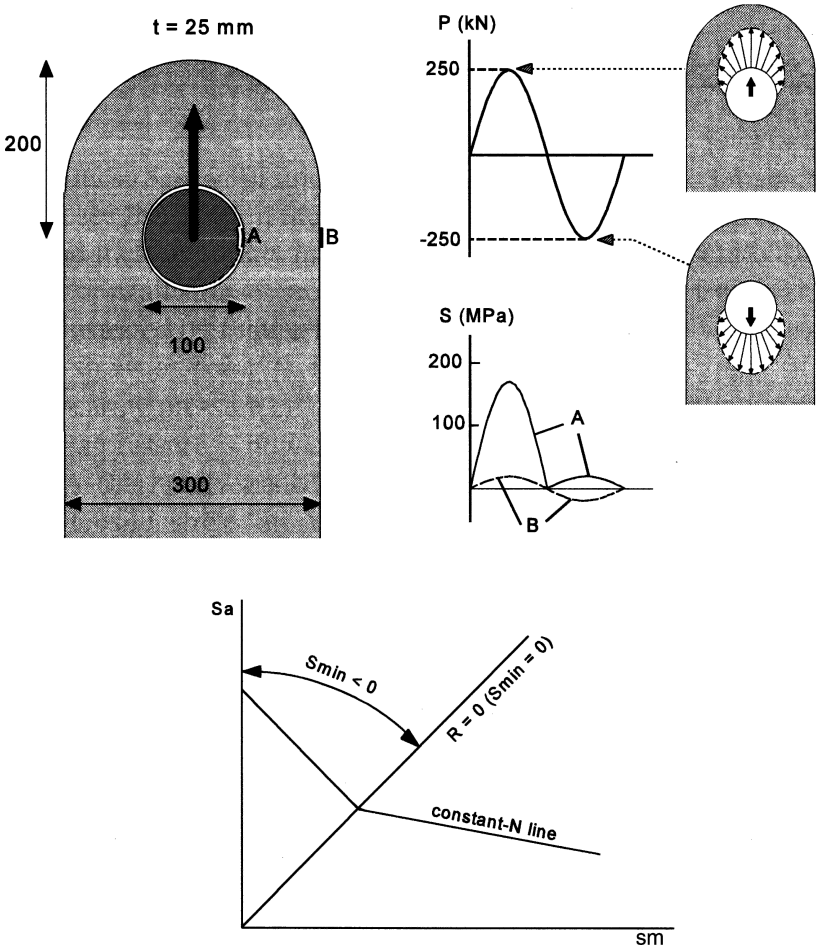

Fig. 18.4 Unusual constant-N lines in the fatigue diagram of lugs due to reversion of the load direction [1].

require fatigue tests on the lug itself. Furthermore, Eq. (18.1) is applicable to positive stresses only; $S_{\min} \geq 0$, or $R \geq 0$.

For negative R-values ($S_{\min} < 0$), lines for constant N-values in the fatigue diagram are abruptly going upward, see the trend in the lower graph of Figure 18.4. This unusual feature is typical for lugs, and it can easily be understood. If the load on a structure is reversed from tension to compression, all stresses are also reversed (Hooke's law). However, this does not apply to lugs as illustrated by Figure 18.4. If a tensile load P is applied to a lug it causes a high tensile peak stress at point A. However, if the load P is reversed from tension to compression, the bearing pressure on the upper

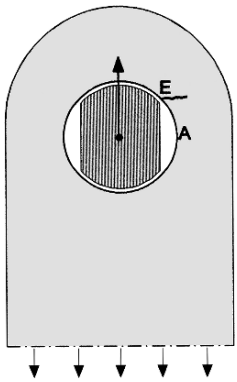

Fig. 18.5 Pin with flats to prevent fretting corrosion at location A of the peak stress [5].

side of the hole disappears instead of being reversed. A bearing pressure is now applied to the lower side of the hole. As a result, the minimum section A-B is hardly loaded. Strain gage measurements have shown that it causes a relatively low tensile stress at A instead of a high compression stress [1]. As a consequence, the peak stress range is not $2K_tS_a$, but only half that value. The nominal fatigue strength increases considerably.

Improvement of the fatigue limit of a lug

The fatigue limit of a lug is very low, see Figures 15.11, 15.12, 18.2 and 18.3. In addition to a relatively high-stress concentration factor, the low fatigue limit is primarily due to fretting corrosion in the hole. The fatigue limit of a lug can be improved in two different ways:

(i) Prevention of fretting corrosion.
(ii) Reduction of the detrimental effect of fretting corrosion damage by introducing compressive residual stresses.

Fretting corrosion is most effectively eliminated by preventing contact between the pin or bolt and the bore of the hole. This can be achieved by slotted holes as discussed in Chapter 15. The results in Figure 15.12 show that a most impressive improvement of the fatigue limit was obtained. Unfortunately, slotted holes are "expensive" holes. Clarke proposed to avoid metallic contact at points A in Figure 18.5 by using pins with flat sides [5]. A worthwhile increase in life was obtained for lugs of an Al-alloy (L65 $\approx$ 2014). A significant increase of the fatigue limit was also reported in [6] for another Al-alloy (7075-T6), while similar improvements were reported

for lugs of some steels [4]. It was observed that cracks in lugs with pins with flat sides started at point E (Figure 18.5). The cracks were still initiated by fretting corrosion, but at a location where the tangential stress is lower than at point A, and the fretting movements are smaller. Obviously, if a pin with flat sides in mounted in a 90° rotated position, the fatigue limit will be reduced rather than improved. Pins with flats should not be considered to be a practical proposition.

Another method for preventing fretting corrosion is by using an interference fit between the pin and lug hole. It was shown by fatigue tests [7] that a hard driven fit increases the fatigue limit, but this is also not a practical solution. Assembling and disassembling of such a joint is no longer feasible. However, a bushing pressed into a lug hole is a good alternative, as already discussed in Chapter 15 (Section 15.4, Figure 15.15). This should be done with a high interference fit in order to prevent fretting movements between the bushing and bore of the hole. The interference fit introduces a high tangential compression stress in the bushing, which suppresses fatigue in the bushing itself. Moreover, the hole in the lug is protected against handling damage caused by mounting and dismounting of bolts or pins.

The fatigue properties of lugs can be much improved by plastic hole expansion, a possibility already discussed in Chapter 4 (Figure 4.7). Plastic hole expansion results in compressive residual stresses in the tangential direction around the hole. The large favorable effect on the fatigue limit of lugs was emphasized in Chapter 15. Fretting damage occurs, but microcracks starting from this damage can be arrested also at relatively high stress amplitudes. The fatigue limit is increased considerably. Plastic hole expansion occurs by pulling an oversized mandrel through the hole, see Figure 4.7. This requires a fairly high pulling force on the mandrel. Moreover, in many practical applications only one side of the component is accessible indicating an apparent need for an expansion technique which can be applied from one side. Two methods were developed for this purpose. The first one is the split-sleeve expansion method developed in the 1970s [8]. The method is illustrated by Figure 18.6. A mandrel is moved through the hole, and then the split sleeve (a bushing with a single split) is moved along the mandrel into the hole. Retraction of the mandrel through the hole and the sleeve in the hole requires a radial expansion of the sleeve and the hole together. As a result, the diameter of the hole is increased by plastic deformation around the hole, and compressive residual stresses in the tangential direction will remain afterwards. A large force is necessary for retraction of the mandrel, but the sleeve has a split and thus the sleeve

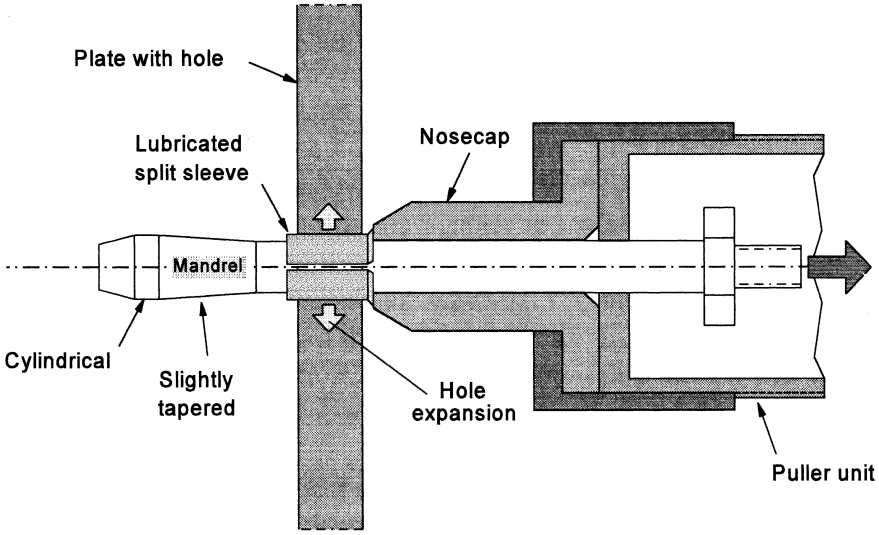

Fig. 18.6 Plastic hole expansion by the split-sleeve method. (Courtesy Len Reid, Fatigue Technology Inc.)

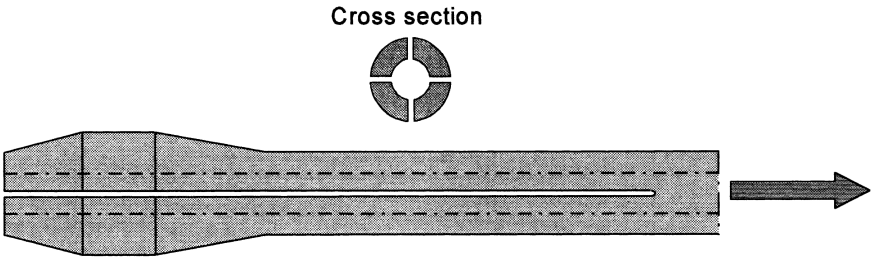

Fig. 18.7 Split mandrel for plastic hole expansion [9].

can easily expand by a small opening of the slit. Furthermore, the friction between the mandrel and the sleeve is reduced by a surface coating baked on the inside of the sleeve. After the mandrel has been retracted, the hole is reamed to the final size and a correct cylindrical shape. The amount of material removed by reaming is small compared to the depth of the plastic zone around the hole. Plastic hole expansion starts from a slightly undersized hole in view of the expansion and subsequent reaming.

The second technique, developed in the 1990s is the split-mandrel method [9]. A mandrel is used with two mutually perpendicular slits along a large part of the mandrel, see Figure 18.7. The maximum diameter is larger than the hole diameter, but the mandrel can still pass through the hole because the slits can be closed by some elastic bending of the four quadrants of

the mandrel. Before retracting the mandrel, a pin is inserted in the center of the mandrel. This prevents closure of the slits during the retraction. The frictional forces between the mandrel and the bore of the hole are reduced by a lubricating oil.

Plastic hole expansion has been successfully applied to many aircraft structures. It is also an attractive method for repair if small cracks occur in service at bolt holes. The bolt is removed, the hole is cleaned and reamed, the hole is plastically expanded and a new bolt with a slightly larger diameter is installed. Successful experience with this rejuvenating repair has been claimed. It is also applied to new aircraft if fatigue problems might be expected. An expansion by 2 to 3% is typical which is sufficient to obtain a significant improvement of the fatigue strength. Larger percentages cause too much lateral deformations and may also introduce some rupture in a material with a fibrous structure. In general, designers are not in favor of plastic hole expansion because of extra costs of manufacturing and quality control.

Plastic hole expansion has also been applied to components of high-strength steels and the Ti-6Al-4V alloy, but the pulling loads are high. Residual compressive stresses were introduced inside large holes in a high-strength steel part of a helicopter by roll-peening. Rollers are forcefully rolled on the material surface inside the bore of the hole which introduces plastic deformation in a way somewhat similar to shot peening. Significant improvements were reported by Waters [10], who found that the fatigue limit for a 4130 lug joint was increased by about 100%.

18.3 Symmetric butt joints with rows of bolts or rivets

A simple double strap joint with two rows of bolts at each side of the joint is shown in Figure 18.8. It appears to be a good design from a static point of view if both rows carry the same load because then $P_A = P_B$ which implies the same bearing pressure on the hole and the same shear stress in the bolts. This will be achieved if the sum of the thicknesses of the two straps is equal to the thickness of the plates: $2t_2 = t_1$. However, from a fatigue point of view, the two rows are in a different position. The holes in row B of the plate are loaded by P_B only. In row A, the same load P_A is present on the holes, but the load already introduced in row B is also passing these holes. The latter load is called a bypass load. With S as the nominal net section stress in the plate, the peak stress at the hole in row A can be written as:

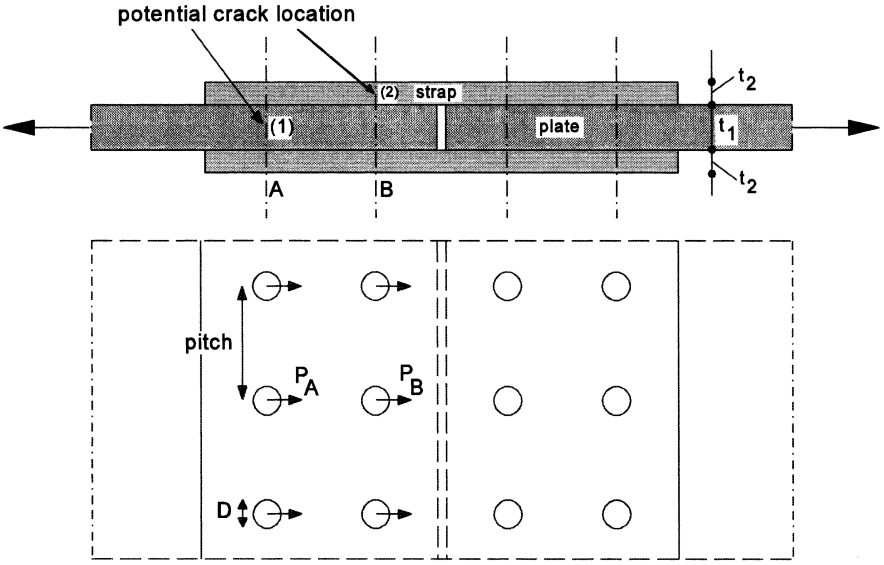

Fig. 18.8 Double strap joint with two rows of bolts (or rivets) at both sides of the joint.

$$(S_{\text{peak}})_{\text{row A}} = \frac{1}{2}S(K_t)_{\text{pin loaded hole}} + \frac{1}{2}S(K_t)_{\text{unloaded hole}} \tag{18.2}$$

The second term is from the bypass load. For row B the peak stress is:

$$(S_{\text{peak}})_{\text{row B}} = \frac{1}{2}S(K_t)_{\text{pin loaded hole}} \tag{18.3}$$

For a ratio of hole diameter to hole pitch of 1/5, the K_t-values of a pin loaded hole and an unloaded hole are 5.2 and 2.5 respectively. Substitution in the two equations gives

$$(S_{\text{peak}})_{\text{row A}} = 3.85S \quad \text{and} \quad (S_{\text{peak}})_{\text{row B}} = 2.6S$$

The results are an approximation because for K_t of the bypass load (unloaded hole) it has been assumed that the hole is an open hole whereas a bolt is present in the hole. Also, the K_t-values do not consider fretting corrosion in the hole. Nevertheless, it is still correct to say that the holes in the plate in row A are more severely loaded than the holes in row B and thus will be more fatigue critical. For the straps, the reverse is true for the same reasons; row B is more fatigue critical than row A. Fatigue cracks occur at either location (1) or (2) in Figure 18.8. Cracks in the plate (location 1) are invisible. It may cause an inspection problem.

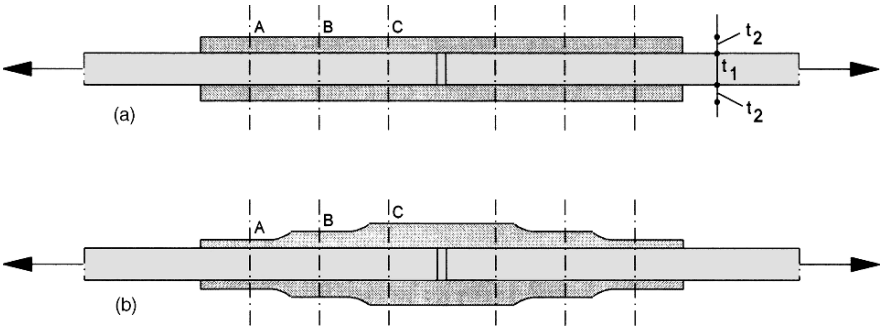

Fig. 18.9 Two double strap joints with a constant and a staggered strap thickness.

Two butt joints with three rows of bolts are shown in Figure 18.9, one joint with a constant thickness of the strap plates, and a second one having strap plates with a staggered thickness. Now, three rows of bolts contribute to load transmission from the plates to the straps. The distribution of the load transmission between the three rows can be obtained by a simple elastic calculation considering equal displacements of bolt holes in the plate and the straps (displacement compatibility). A surprising result is obtained for the joint with the constant-thickness straps in Figure 18.9a again with $t_2 = t_1/2$. The result of the simple displacement compatibility analysis is that $P_A = P_C$ and $P_B = 0$; in other words, the middle row of bolts does not contribute to load transmission. This can easily be understood by considering that the strain between A and C is constant and equal in the plate and the two straps. It implies that the displacements of the holes at B in the plate and in the straps are equal and thus the bolts in row B remain unloaded. A more elaborate FE calculation will indicate that the bolts of the second row carry some load, but still much less than the bolts in the other two rows.[23]

A better distribution of load transmission between the three rows is obtained by staggering the thickness of the straps, see Figure 18.9b. This can be done in such a way that $P_A = P_B = P_C$. However, it is true again that the bolt holes of row A in the plate are the more fatigue critical holes because of the maximum bypass load in addition to the pin-loading. This is called the end-row effect because row A is the last one in the plate. The end-row effect on fatigue can be reduced by designing the staggered strap for a lower load transmission than 1/3. Such improvements are obtained by local variations of the stiffness of the joint.

[23] Under static load until failure, the bolts in row B will significantly contribute to load transmission because plastic deformation around the holes will lead to a more homogeneous load distribution between the three rows.

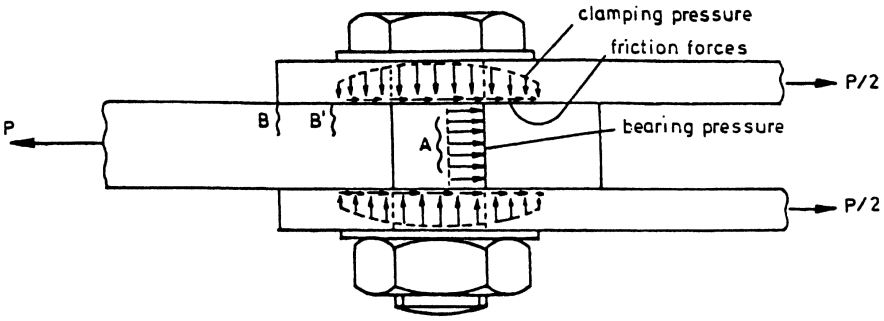

Fig. 18.10 As a result of clamping, load transmission also occurs by friction forces. Shift of crack location is possible.

Clamping bolts of a joint

Bolts can be pre-tensioned by controlled torque with a torque wrench. This can have a large impact on the fatigue life. Load transfer from one element to another one now occurs partly by frictional forces. Moreover, the coefficient of friction, which statically may be in the order of 0.3 for a dry assembling, can increase considerably under cyclic load as a result of fretting between the clamped plates. If clamping is absent, fatigue cracks are initiated at the edge of the hole in the net section, see location A in Figure 18.10. However, after sufficient tightening of the bolt, fretting movements inside the hole are suppressed. Crack initiation shifts to locations B or B′. Clamping will increase the fatigue strength until this shift of the crack location has occurred. More clamping should not give a further improvement.

18.4 Bolts loaded in tension

Bolts loaded in tension are frequently used in structures because it allows easy assembling and disassembling. If a tension bolt is subjected to cyclic loading it should be admitted that the shape of a bolt is poor from a fatigue point of view. Significant stress concentrations occur in a bolt at three locations, see Figure 18.11:

1. At the transition from the bolt head to the shank of the bolt.
2. In the groove between shank and screw thread (not always present).
3. In the screw thread.

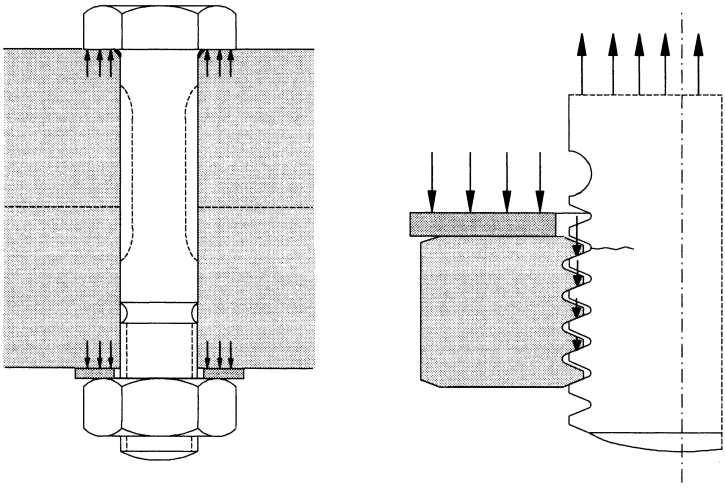

Fig. 18.11 Tension bolt with loads on bolt head, washer and screw threads between nut and bolt.

The bolt head is loaded in an unfavorable way because the load is applied close to the root of the notch. A similar case was discussed in Chapter 3 for a flat anchor bolt (T-head), see Figure 3.18 with high K_t-values. The circular cross section of a normal bolt will give a somewhat lower stress concentration. Unfortunately, the radius between the bolt head and shank cannot be made large in view of interference with the hole edges. Values of K_t of the order of three and even larger are possible. The bottom plane of the bolt head and the plate to be clamped should be perfectly parallel because otherwise the bolt head is also loaded in bending. This can be disastrous for fatigue.

In general, the groove between the shank and screw threads will not be critical because the radius is larger than the root radius in the screw thread itself, see the cross section in Figure 18.11. The root radii of the screw threads are standardized, unfortunately at low values leading to a significant stress concentration. Furthermore, the load transmission from the bolt to the nut is not homogeneously distributed over the screw threads. As indicated in Figure 18.11 by the arrows on the screw threads, the largest contribution to the load transmission occurs by the first full screw thread of the nut. As a result, fatigue cracks initiate at the corresponding screw thread of the bolt, the more so because the loads of the other screw threads also pass through this cross section (bypass load). Most fatigue failures occur at this location of the bolt.

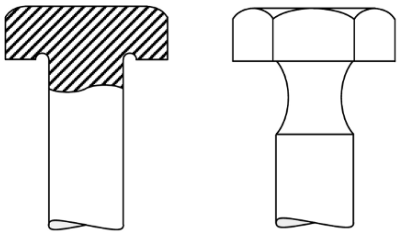

Fig. 18.12 Modified bolt heads to reduce the stress concentration between bolt head and shank.

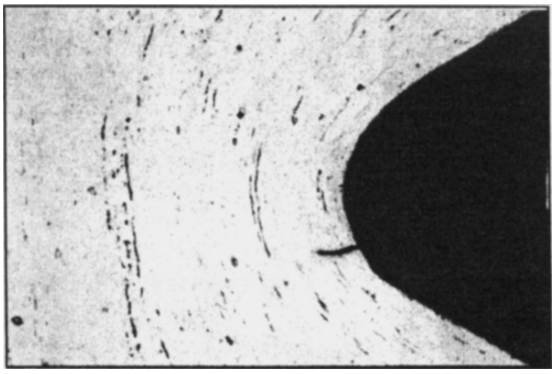

Fig. 18.13 A small fatigue crack in the screw thread of a bolt. Crack length 40 μm. Note the structure of the rolled screw thread as revealed by the curved pearlite strings [14].

Several possibilities have been proposed to improve the bolt design, see e.g. [11–13]. Two possibilities to reduce the root radius between the bolt head and shank are shown in Figure 18.12. The local K_t-value can thus be reduced. Improved screw thread concepts for bolts and nuts were also proposed. However, special bolts and nuts are not generally appreciated to avoid fatigue problems. Designers prefer to rely on high-quality bolts and pre-tensioning the bolt. High quality bolts are made of low-alloy steel which allows a high pre-tension in the bolt.

The screw thread of a bolt is made either by cutting or rolling. It should be recommended to use rolled thread for fatigue loaded bolts. A cutting operation cuts through the fibrous structure of the material, whereas rolling will force the fibrous structure to follow the thread profile, see Figure 18.13. Moreover, rolling leaves a better surface quality and can also introduce residual compressive stresses at the root of the screw thread. High-quality bolts always have rolled threads. The fatigue strength, and especially the fatigue limit are much better than for bolts with cut screw thread.

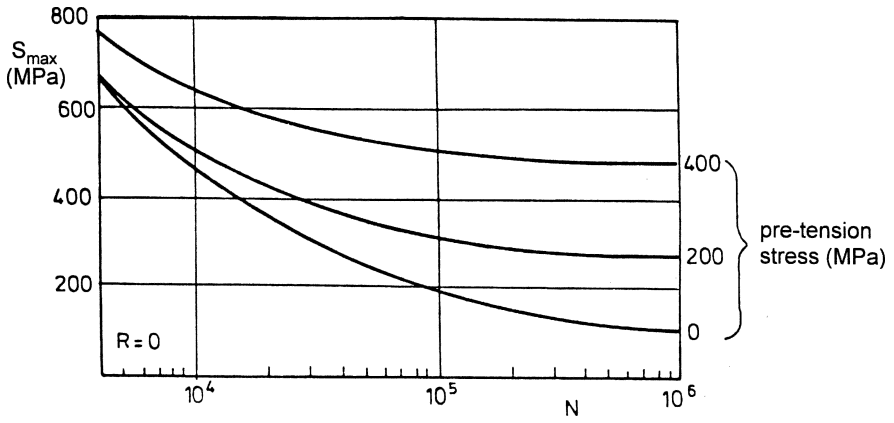

Fig. 18.14 Effect of pre-tension on the S-N curve of a steel bolt loaded in tension (diameter 10 mm) [15].

Pre-tension in bolts

During assembling of a bolted structure, it is usual to tighten a bolt by applying a prescribed torque moment to the nut. This introduces a pre-tension load in the bolt. If a cyclic load is applied to the structure, the pre-tension increases the mean stress in the bolt, but reduces the stress amplitude. In view of the predominant effect of the stress amplitude, a significant gain of the fatigue strength can be obtained. This is illustrated by the S-N curves in Figure 18.14.

The mechanism of pre-tension in the bolt can be explained with reference to Figure 18.15. In this figure two parts A and B are clamped by a pre-tensioned bolt. The pre-tension load in the bolt is causing a compressive load on the contact area between the two parts (P_{contact}). In the unloaded joint $P_{\text{contact}} = -P_0$, with P_0 as the pre-tension load of the bolt. If a load P is applied on the joint, the load in the bolt (P_{bolt}) will increase, and P_{contact} will become less compressive. However, the joint is still reacting as an integral part as long as contact between the two parts does exist. It implies that the load transmission in the joint occurs partly as load flow through the bolt and for another part via the contact area. The load increment in the bolt will thus be smaller than the increment of the applied load. The simple equation with load increments is:

$$P = \Delta P_{\text{bolt}} + \Delta P_{\text{contact}} \tag{18.4a}$$

or

$$\Delta P_{\text{bolt}} = P - \Delta P_{\text{contact}} \tag{18.4b}$$

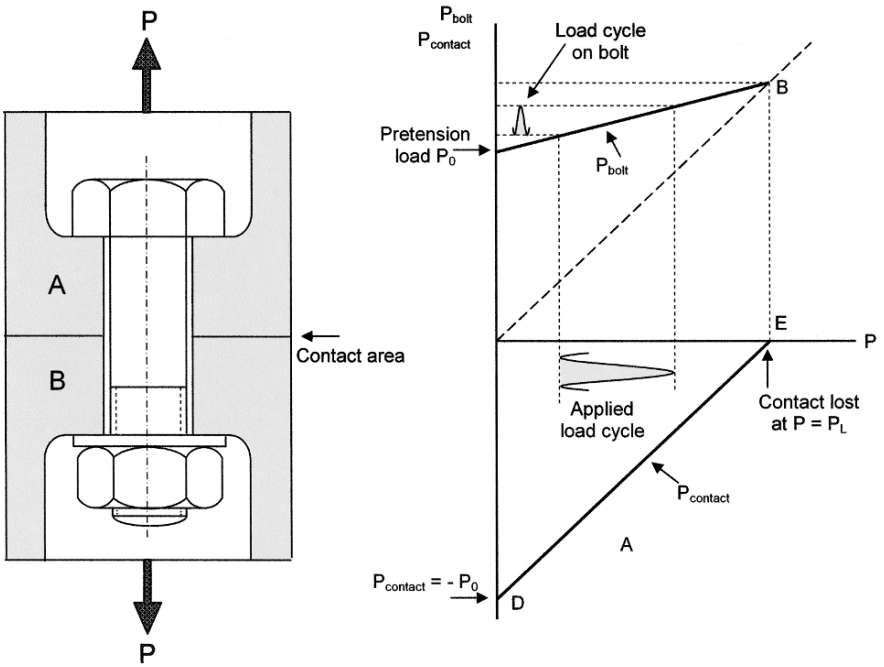

Fig. 18.15 Increased mean load and reduced load amplitude by pre-tension of bolt.

During an increasing load P the contact load will become smaller, which means that P_{contact} becomes less negative, and thus $\Delta P_{\text{contact}}$ is positive. Thus,

$$\Delta P_{\text{bolt}} < P \tag{18.5}$$

The effect of pre-tension on the reduction of the incremental load in the bolt is further illustrated in Figure 18.15. Both P_{bolt} and P_{contact} are plotted along the vertical axis as a function of the load P applied on the joint along the horizontal axis. If the load P is increased, the contact load starting at $P_{\text{contact}} = -P_0$ will become smaller until $P_{\text{contact}} = 0$ at point E in Figure 18.15. The corresponding load is denoted as P_L. For $P > P_L$ contact between parts A and B is lost. During the same increasing load from $P = 0$ to $P = P_L$, the load in the bolt starts at the pre-tension load P_0 and increases to $P = P_L$. It turns out that the load variation in the bolt is significantly smaller than the load applied on the joint. The consequence for a cyclic load is illustrated in Figure 18.15 by a specific applied load cycle and the corresponding load cycle in the bolt. As said before, pre-tensioning of the bolt increases S_m in the bolt but a significant reduction of S_a is obtained which has a predominated effect and the fatigue strength as illustrated by the

results in Figure 18.14. However, if $P > P_L$ then the contact between the two connected parts is lost, and P_{bolt} will be equal to the applied load.

The pre-tension effect can be enhanced by reducing the stiffness of the bolt. If the stiffness coefficients of the bolt and the compressed material of the joint are denoted by C_{bolt} and C_C respectively, and the elongation of the bolt by $\Delta\ell$, then

$$\Delta P_{\text{bolt}} = C_{\text{bolt}}\Delta\ell, \quad \Delta P_C = C_C\Delta\ell \tag{18.6}$$

Substitution in Eq.(18.4) gives:

$$\frac{\Delta P_{\text{bolt}}}{P} = \frac{1}{1 + C_C/C_{\text{bolt}}} \tag{18.7}$$

According to this equation, a lower C_{bolt} will reduce ΔP_{bolt}, and the favorable effect of pre-tensioning increases. A lower C_{bolt} can be obtained by using a waisted bolt, see the dotted lines in Figure 18.11. Another option is to use a bolt of a Ti-alloy which has a lower E-modulus than steel. These bolts are used in aircraft, also because of weight-saving.

Pre-tensioning is effective as long as separation at the contact area of the joint does not occur. For this reason, high-strength steel bolts are pre-tensioned to a high stress level up to 70% of $S_{0.2}$ (P_0 calculated for the minimum diameter of the screw thread). This also helps to come to a more uniform load transfer along the screw thread of the bolt. Usually, the pre-tension is controlled by tightening of the nut with a calibrated torque wrench. However, the relation between the torque moment and the pre-tension load in the bolt is strongly dependent of the friction between the nut and washer and between the screw threads of nut and bolt during tightening of the bolt. Lubrication should be considered because it gives a larger pre-tension in the bolt for the same torque moment. For critical tension bolts, special means are available to assure that the required pre-tension has been installed. This can be done by measuring the length increment of the bolt, but also by using special washers.

It is important to emphasize that the favorable effect of pre-tensioning is fundamentally different from the favorable effect of compressive residual stresses obtained by shot peening or plastic hole expansion. Residual stresses reduce S_m and do not affect S_a, whereas pre-tensioning increases S_m and reduces S_a.

18.5 Riveted and bolted joints with eccentricities

Single lap joints between sheets are used in various structures. Overlapping sheets are joined by a number of fasteners (rivets or bolts). The variety of such joints is large; the material, material thickness, type of fastener, pattern of fastener locations (how many rows, and how many fasteners in a row), hole diameters, distances between fasteners, joining techniques, etc. Some essential aspects with respect to fasteners should be mentioned.

Bolts usually have a clearance fit in the hole, while clamping between the sheets can be controlled by tightening of the bolts. Riveting occurs by a deformation process on the rivet to fill up the hole and to produce the closing head (also called the driven head). Solid rivets are usually of a similar alloy as the sheets or plates. Riveted joints were applied already long ago in steel structures (e.g. bridges, cranes, ships, etc.) and also in aluminium structures, in particular aircraft structures. Riveting occurs by hammering or squeezing. Squeezing is not noisy, in contrast to hammering. Moreover, squeezing can be done in an automated production process which gives a more uniform production quality.

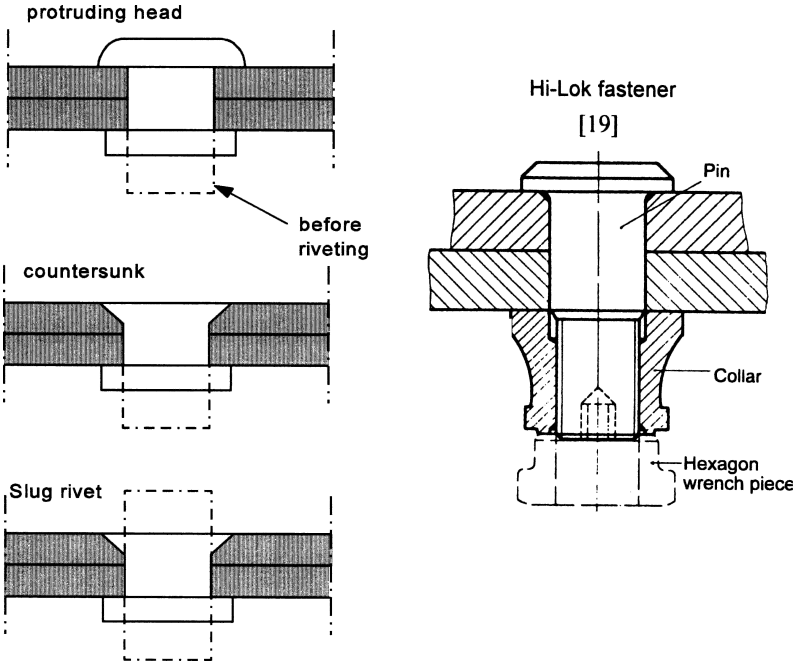

Fig. 18.16 Different types of fasteners.

A few fastener types are shown in Figure 18.16. The protruding head rivet is the older one, which is also often used with a spherical head. The countersunk rivet was introduced to obtain a flat surface at one side of the joint which can be desirable for aerodynamic or hydrodynamic reasons. Due to the countersunk hole, the stress concentration at the hole is larger than for the cylindrical hole of a protruding head rivet [16]. During riveting, the force applied on the rivet is pressing material of the rivet shank into the rivet hole. Hole filling depends on the rivet force, which is also called the squeeze force. If the force is low, the hole is just filled up, but if a larger force is used, the hole is plastically expanded and a much better contact between the entire rivet and the hole is obtained. This leads to better fatigue properties as discussed later.

Several types of fasteners were developed for aircraft applications for special reasons, e.g. easy and fast assembling, good fatigue properties, and high static shear strength [17]. An example is the Hi-Lok fastener also shown in Figure 18.16. It is usually installed with a slight interference fit for good hole filling. The fastener is made from a high-strength steel or Ti-alloy to obtain a large static shear strength. The installation of the nut on the bolt is done from one side. The nut consists of two parts, a collar which is the real nut, and a hexagon wrench piece, see Figure 18.16. During installation, the hexagon piece is tightening the nut until this piece is sheared off from the nut. As a result, a well-controlled high torque is applied which ensures a significant clamping of the sheets by the Hi-Lok fastener, and also a high strength and good fatigue properties. Of course such a fastener is more expensive than a conventional rivet or bolt. A variety of high-tech fasteners is commercially available [18, 19].

Some simple types of riveted joints with eccentricities are schematically indicated in Figure 18.17; three lap joints with 1, 2 and 3 rows of fasteners respectively, and a single-strap butt joint with four rows of fasteners. Actually, the latter joint can also be identified as two lap joints in series with two rows of fasteners each. The eccentricities of the joints imply that the neutral line is not a straight line but contains one or more eccentricities, see Figures 18.18 and 18.19 to be discussed later. Symmetric double strap joints shown earlier (Figures 18.1 and 18.9) do not have such eccentricities. Characteristic differences occur between joints with and without eccentricities:

1. The fasteners in a single lap joint are single-shear fasteners loaded in shear in one cross section of the fastener only. The fasteners in a double strap joint are double shear fasteners with two cross sections equally

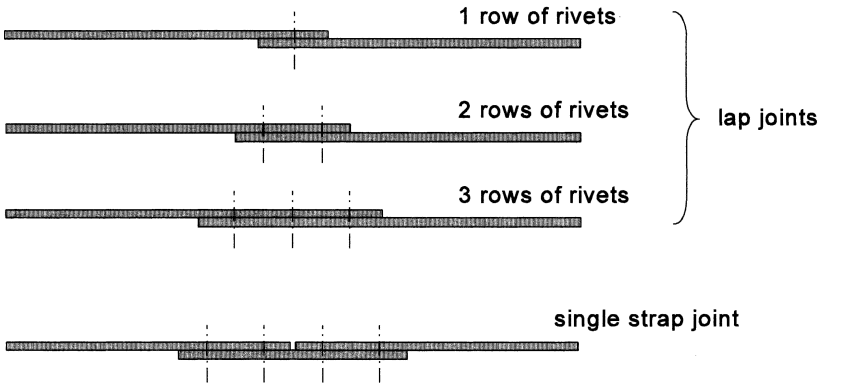

Fig. 18.17 Different types of simple riveted joints with eccentricities at the rivet rows.

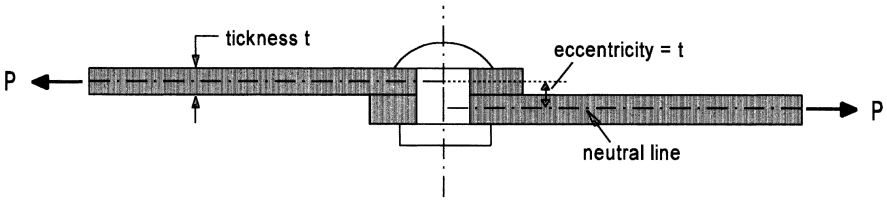

Fig. 18.18 Lap joint with one row of rivets. Large eccentricity at rivet row.

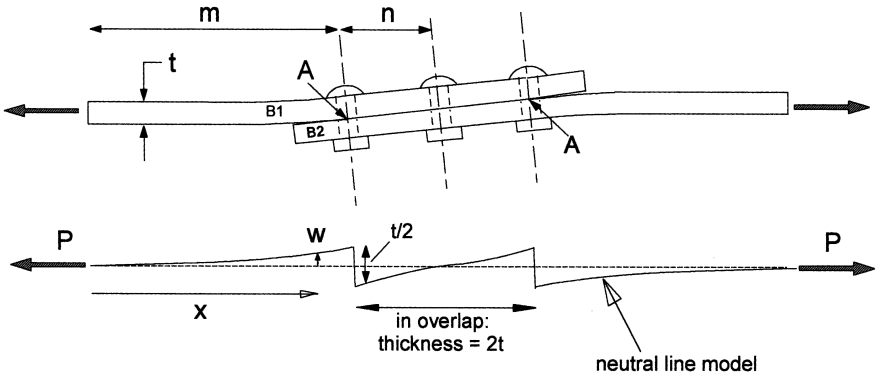

Fig. 18.19 Secondary bending in a riveted lap joint under tensile loading.

loaded in shear. As a result, the shear strength of a double strap joint is larger.

2. In a lap joint, only one contact surface is present between the two plates or sheets of the joint. Load transmission by frictional forces can occur in one mating surface only. In a double strap joint, two such mating planes are available which is favorable for the load transmission.

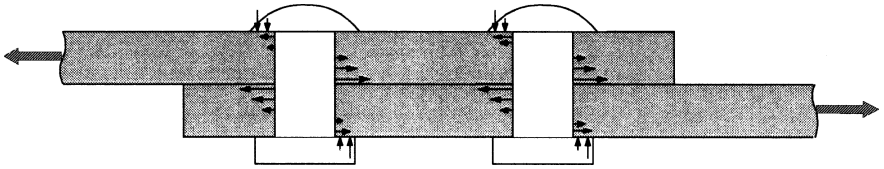

Fig. 18.20 Asymmetric loading on rivets as a result of the eccentricity in a lap joint.

3. As a result of the eccentricities in a lap joint, a tensile load on the joint causes bending of the plates, see Figure 18.19. Maximum bending stresses occur at the eccentricities, i.e. at the fastener rows (point A in Figure 18.19). This will cause an extra stress concentration at the holes of the fasteners. Bending caused by the tensile load is referred to as *secondary bending*. It is a by-product of the tension load.
4. The fastener in a lap joint is asymmetrically loaded, see Figure 18.20, and the fastener will tilt in the hole if the hole filling by the fastener is poor. This gives an inhomogeneous bearing pressure along the hole.

All aspects (1) to (4) are unfavorable for the joint with eccentricities in comparison to symmetric joints without eccentricities. An obvious eccentricity occurs in a riveted lap joint with a single row of rivets. The eccentricity is equal to the sheet thickness, see Figure 18.18.

The bending moment at the rivet row in Figure 18.18 is equal to $Pt/2$, which leads to the following bending stress:

$$S_{\text{bending}} = \frac{\frac{1}{2}Pt}{\frac{1}{6}Wt^2} = 3\frac{P}{Wt} = 3S_{\text{tension}} \tag{18.8}$$

(W = width of joint). Both S_{bending} and S_{tension} are nominal stress levels, disregarding the presence of the holes filled with rivets. The bending factor, k, is defined as the ratio of the bending stress and the tensile stress:

$$k = \frac{S_{\text{bending}}}{S_{\text{tension}}} \tag{18.9}$$

For the single rivet-row lap joint, $k = 3$ according to Eq. (18.8). The bending stress is three times the tension stress, which is a significant increase of the stress level at the critical location of the joint. The fatigue strength of riveted lap joints with a single rivet row is poor indeed. The fatigue strength of riveted lap joints with two or more rivet rows is significantly better. Bending is less, and furthermore, the load transmission occurs in more than one rivet row.

The secondary bending caused by the tension load can be calculated by considering the out-of-plane displacements of the neutral line of the joint, denoted by w, see Figure 18.19. It leads to a differential equation for the bending moment M_x:

$$M_x = Pw = E^* I \frac{\mathrm{d}^2 w}{\mathrm{d}x^2} \tag{18.10}$$

$E^* = E/(1 - \nu^2)$, E is Young's modulus, ν is Poisson's ratio,[24] I is the inertia moment of the cross section of the sheet. The solution of the equation, using boundary conditions and assuming that the length m in Figure 18.19 is much larger than n, leads to Eq. (18.11) for the bending factor. The derivation is given in [20].

$$k = \frac{3}{1 + 2\sqrt{2}\, T_2} \text{ with } T_2 = \tanh\left(\frac{n}{t}\sqrt{1.5\frac{S}{E^*}}\right) \tag{18.11}$$

(t is the sheet thickness, $2n$ is the row distance for a specimen with two rivet rows, and n is the row distance if three rivet rows are present; tanh is the hyperbolic tangent function). It should be noted that the bending factor depends on the applied tensile stress S. The relation between S_{bending} and S is non-linear, which is illustrated by the calculated results in Figure 18.21 for a lap joint with three rows of rivets. The bending factor in this case is $k = 1.36$ at $S = 100$ MPa which is considerably lower than the extreme $k = 3$ for the single-row lap joint. For a three-row lap joint with the same row distance, the calculated bending factor, again at $S = 100$ MPa, is reduced to $k = 0.99$. This reduction is not a consequence of having three rows of rivets, but it is due to a two times longer overlap. Fatigue tests on riveted lap joints with two rows of rivets have shown that the fatigue life is improved by increasing the distance between the two rows [21].

A comparison of S-N curves of three different types of riveted joints is made in Figure 18.22. Obviously, the symmetric butt joint without any secondary bending is superior to the other two types of joints. The bending factor k for the lap joint and the single-strap butt joint are $k = 1.78$ and 2.40 respectively (calculation data $t = 1.2$ mm, $n/t = 5.42$, $E = 72000$ MPa for the 2024-T3 Al-alloy, and $S = 100$ MPa). Equation (18.11) is not valid for the single strap joint, but again a similar k equation was derived with

[24] In the previous edition of this book prevention of anti-clastic bending was ignored, and thus E^* was simply assumed to be equal to E. In general, some prevention of anticlastic bending will be present in thin sheets which will cause a small increase of the bending stiffness. Secondary bending calculations with the neutral line model but ignoring anticlastic bending may yield a slightly larger bending stress, in the order of 10% larger.

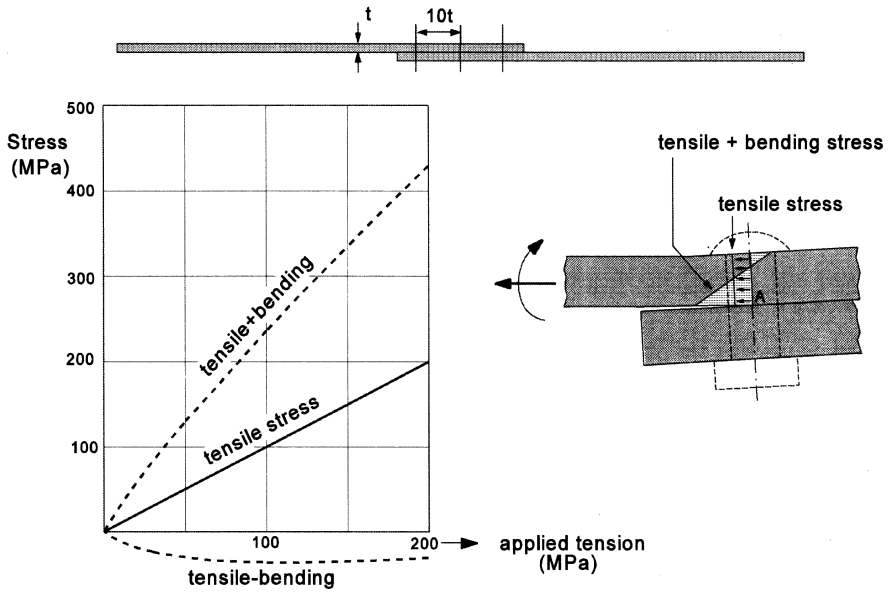

Fig. 18.21 Non-linear secondary bending stresses in a riveted lap joint calculated with Eq. (18.14) for Al-alloy sheet material.

Eq. (18.10). The higher k factor of the single strap joint has indeed led to a lower S-N curve.

The most critical points for crack initiation in a riveted lap joint are points A of the first and last row of the joint indicated in Figure 18.19. To a certain extent, this is the end-row effect discussed before for symmetric bolted joints. However, the effect is still aggravated in a lap joint because of the additional bending stress caused by secondary bending. The maximum bending stress occurs at the same end rows, see point A in Figure 18.21. Furthermore, fretting corrosion between the two sheets cannot be avoided. In Figure 18.19, part B1 of the left sheet carries the full load on the joint, whereas part B2 of the other sheet is unloaded. Fretting between the two sheets occurs, especially around the rivet holes of the end rows. The superposition of stress concentration, secondary bending and fretting corrosion explains why the fatigue limits of the S-N curves in Figure 18.22 are low.

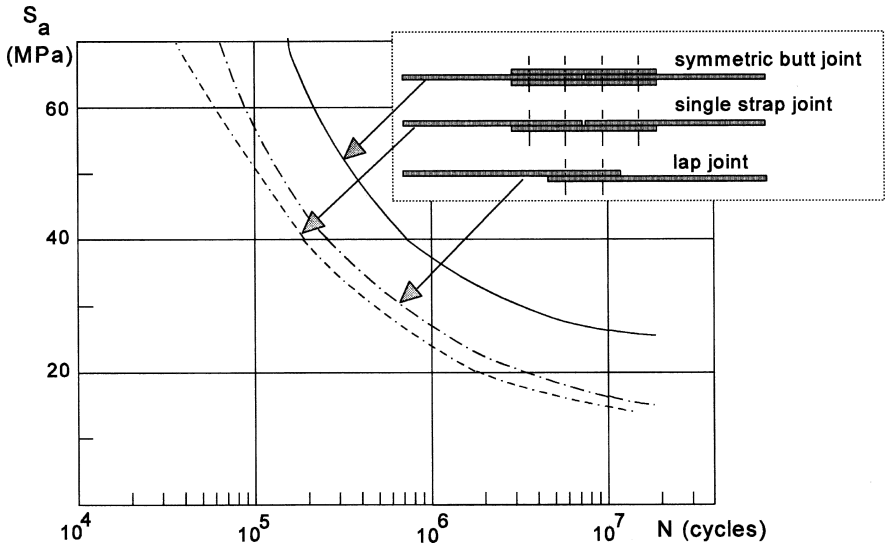

Fig. 18.22 Fatigue curves for three different types of riveted joints. Material 2024-T3 Alclad ($t = 1.2$ mm), $S_m = 69$ MPa [21].

Effect of the rivet squeeze force

As emphasized earlier, the load transmission in a riveted joint is a complex phenomenon. Hole filling has been mentioned as a significant aspect. The shank of a fastener should fully fill up the hole, preferably with an interference fit. This will prevent rivet tilting and the related unfavorable pressure distribution of the rivet on the hole. The shear deformation of the rivet and the surrounding material (rivet flexibility) will be reduced by an improved hole filling. Furthermore, the fatigue sensitivity for the surface finish of the hole will be less.

Hole filling in a riveted joint depends on the plastic deformation of the rivet during the riveting process. It can be improved by increasing the squeeze force on the rivet during riveting. If this force is sufficiently large, the rivet hole will be expanded and an interference fit is obtained. The shank of the rivet is then surrounded by pre-tensioned sheet material. Measurements of the deformation of the driven rivet head as a function of the squeeze force are given in Figure 18.23. The height of the driven head is decreased and the diameter is increased by a larger squeeze force, as should be expected. At the same time, hole expansion is introduced up to a few percent. The favorable effect of a high squeeze force on the fatigue life is shown by Figure 18.24.

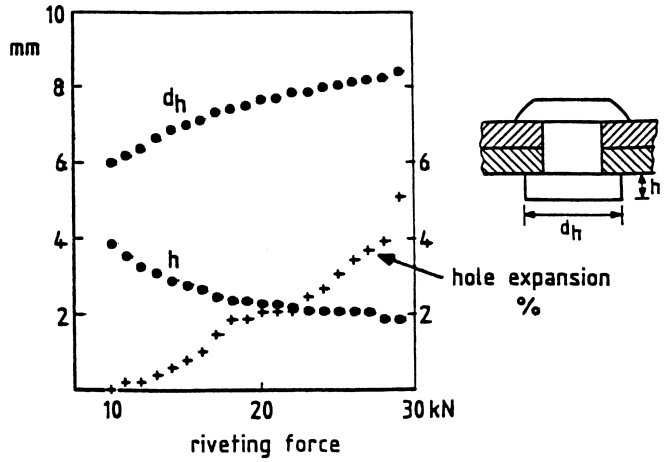

Fig. 18.23 Deformation of the driven rivet head and hole expansion as a function of the rivet squeeze force [22].

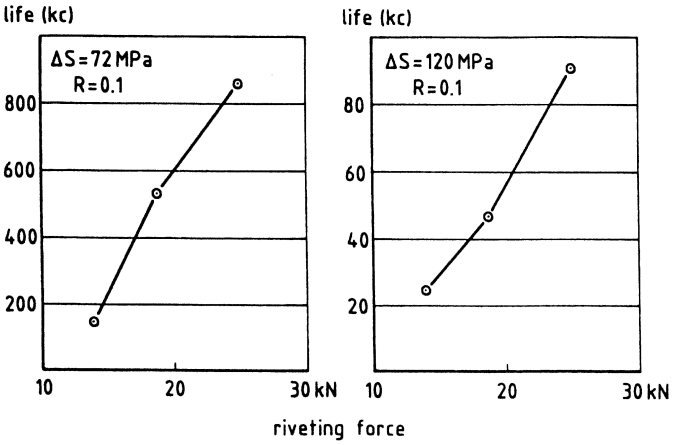

Fig. 18.24 The effect of the rivet squeeze force on the fatigue life of a riveted lap joint. Material: Al-alloy 2024-T3, $t = 2$ mm, rivet diameter 4.8 mm, $R = 0$ [22].

Apparently, a significant increase of the fatigue life can thus be achieved. More results are presented in [23].

An increased squeezing force will also increase the clamping force of the rivets on the sheets. Clamping of the rivets affects the location of the fatigue crack. If the clamping is poor, cracks start at the rivet holes in the minimum section of the most critical end row, i.e. at point A in Figure 18.25. Such a crack is shown in Figure 18.26a. Fretting at that location causes crack initiation. However, if an improved clamping is obtained, fretting movements

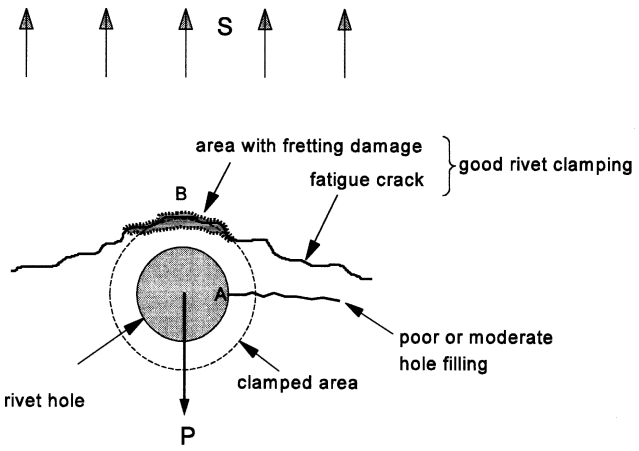

Fig. 18.25 Crack initiation at B outside rivet hole [22].

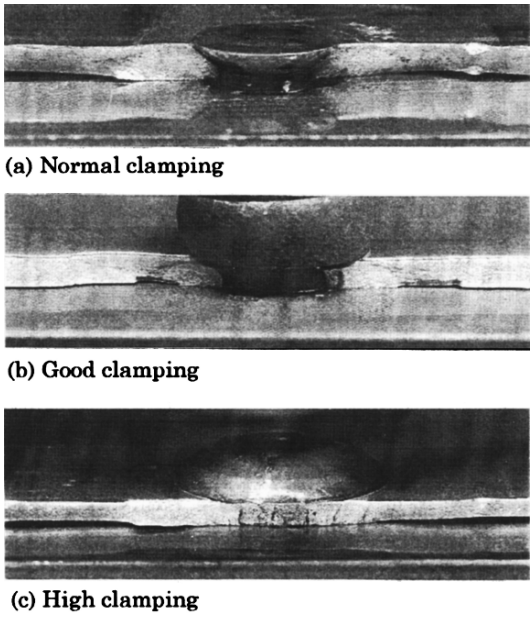

Fig. 18.26 Effect of clamping on fatigue crack at rivet holes [22]. (a) Corner cracks at hole edge. (b) Semi-elliptical cracks slightly away from hole. (c) Crack growing around hole.

are no longer possible near the hole. Crack nucleation starts still in the minimum section by fretting between the two mating surfaces, but it occurs slightly outside the hole, see the semi-elliptical cracks in Figure 18.26b. With a further increase of the squeezing force the clamping of the two sheets by the rivet becomes considerable. Fretting around the hole is highly

restrained, but it cannot be prevented at the edge of the clamped area near point B in Figure 18.25 where secondary bending is large which implies that some separation between the two sheets must occur. Several crack nuclei are created simultaneously which are linked up to a single crack with a ragged appearance, see Figure 18.26c. This crack no longer grows through the hole, but around the rivet hole. The phenomenon is somewhat similar to the effect of bolt clamping as described earlier, see Figure 18.10, although secondary bending is not involved in the symmetric joint.

Predictions on the fatigue life of riveted lap joints

Predictions of the fatigue life of a riveted lap joint should be expected to be a complex problem in view of secondary bending, fastener type, fretting corrosion and rivet hole filling; all having a significant effect of the fatigue life. These aspects are not easily accounted for by analytical equations. Moreover, geometric variables of the joint must also be considered. Homan and Jongebreur [24] suggested a prediction method for riveted lap joints in sheet material of aircraft fuselage structures loaded under constant-amplitude loading. The model starts from an S-N curve of a reference lap joint for $R = 0$ for which fatigue data are available. Predictions are extrapolated from this curve by accounting for three contributions to the stress concentration at the rivet holes of the critical end row. The contributions are associated with (i) load transmission by the rivets (pin loading on the hole), (ii) bypass loading of the other rivet rows, and (iii) increased stress by secondary bending. The equation used is the following:

$$K_t = \gamma K_{t,\text{pin}} + (1 - \gamma) K_{t,\text{hole,tension}} + k K_{t,\text{hole,bending}} \tag{18.12}$$

In this equation, γ is the percentage of the load transmitted to the other sheet in the critical row. Then, $(1 - \gamma)$ is the percentage of the bypass load. The factor k is the secondary bending factor as defined in Eq. (18.9). The three stress concentration factors, $K_{t,\text{pin}}$, $K_{t,\text{hole,tension}}$ and $K_{t,\text{hole,bending}}$, depend on the joint geometry (rivet diameter/rivet pitch). It may be noted that Eq. (18.12) is partly similar to Eq. (18.2) for a symmetric butt joint with two rows of fasteners. The secondary bending term does not occur in Eq. (18.2), and γ of Eq. (18.12) is equal to 0.5 in Eq. (18.2).

The prediction method of Homan and Jongebreur is based on the peak stress calculated with Eq. (18.12). The peak stress is calculated for the reference joint and for the actual joint for which life predictions should be made. The similarity principle is adopted, which implies that similar peak

stresses in the reference joint and the actual joint should give similar fatigue lives. Obviously, the fastener type, fretting corrosion and rivet hole filling are not accounted for by Eq. (18.12). As pointed out by Homan and Jongebreur, these conditions should be similar for the reference joint and the actual joint. If this similarity is questionable, more relevant reference data should be used. It might well imply that fatigue tests have to be made on the actual joint.

18.6 Adhesive-bonded joints

Adhesive bonding is widely used for various technical applications, including metal-to-metal bonding and bonding of a metallic material to a non-metallic material. If bonding of metals is done under closely controlled conditions, high-quality and durable joints can be made. Structural applications with a primary load on the adhesive bond line are still largely restricted to aircraft structures. Tensile loads on an adhesive metal-to-metal bond line are generally avoided because of the possibility of peeling failures.[25] However, the static strength and fatigue strength under shear loading are satisfactory.

In principle, adhesive bonding of Al-alloy sheet material in a lap joint should be attractive if compared to a riveted lap joint. In order to see the advantages of adhesive bonding with respect to fatigue, two fundamental differences between the two types of lap joints are important. First, in a riveted lap joint, the overlapping sheets are attached to one another at discreet points only, i.e. by the fasteners. Obviously, severe stress concentrations should occur. However, if the attachment is made continuously in the full overlapping area by adhesive bonding, these stress concentrations do not occur. Secondly, metallic contact between the two sheets is absent in the adhesively bonded joints, and thus fretting between the mating sheets is also eliminated. From a fatigue point of view, adhesive bonding is the preferred jointing method. Fatigue tests have confirmed this conclusion as shown by the S-N curves in Figure 18.27. It should also be noted that the nominal overlap of the two types of specimens in Figure 18.27 are the same, but the effective overlap is larger in the bonded lap joint (60 mm) than in the riveted lap joint (40 mm = distance between two outer rows). As previously mentioned, the larger overlap reduces secondary bending.

[25] In the literature, a peeling failure is often associated with the mode I opening as defined in Figure 5.2. The peeling resistance can still be satisfactory if a good adhesive is used in accordance with the prescribed bonding operation.

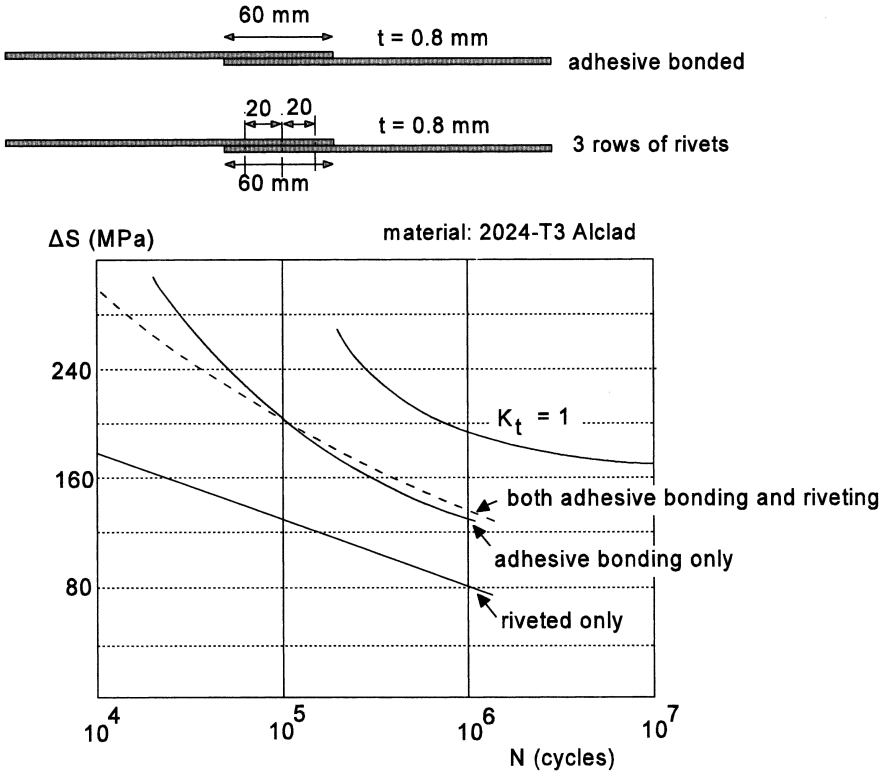

Fig. 18.27 S-N curves of bonded lap joints ($R = 0.1$). Comparison to the S-N curve of a riveted lap joint with a similar geometry, and to the S-N curve of unnotched material [25].

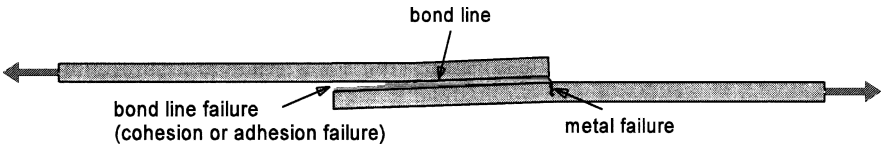

Fig. 18.28 Two different failure modes in an adhesive-bonded joint.

Two fatigue failure modes of an adhesive bonded lap joint are shown in Figure 18.28. Under high-load amplitudes and with a short overlap (e.g. 10 times the sheet thickness or less), failures can occur in the bond line, either in the adhesive itself (cohesion failure) or at the interface between the adhesive and metal (adhesion failure). This will depend on the quality of the pre-treatment of the metal surfaces, adhesive and curing cycle. The quality of the adhesives and the bonding techniques have been much improved, and short overlaps are not used. As a result, sheet metal failure is the

predominant fatigue failure mode. The sheet metal failure is the result of the stress concentration at the end the overlap and the occurrence of secondary bending with the maximum bending factor at the same location. An abrupt thickness variation is present at the end of the overlap. A significant stress concentration might be expected, but it is less serious because of the low elastic modulus of the adhesive. Young's modulus is of the order of 3000 MPa compared to 72000 MPa for the aluminium alloy sheet material. The bond line thickness is usually in the range of 0.1 to 0.2 mm. Contrary to intuition, the bond line thickness seems to have a minor influence on the fatigue strength.

18.7 General discussion on predictions of fatigue properties of joints

Fatigue of a variety of joints has been discussed in the previous sections. Apparently, each type of joint has its own specific features depending on how the load transmission occurs in the joint. Several phenomena were revealed, such as fretting corrosion, clamping, secondary bending, bypass loads, which all can affect the fatigue properties. Unfortunately, it turned out to be difficult to account quantitatively in a fully rational way for these influences on the fatigue life. Joints do not allow such simple comparisons as discussed in Chapter 7 on elementary notch geometries fully characterized by K_t, the size of the notch root radius and surface roughness. In the latter case, the fatigue properties were predicted with the fatigue data of unnotched specimens as basic reference data. Although these predictions also had limitations, the similarity concept could still be used. The logic of the similarity concept was: similar conditions in notched components and unnotched specimens should lead to the same fatigue properties. Such a simple similarity cannot be defined for joints due to the more complex conditions of joints. The prediction techniques discussed in the previous sections all start from available fatigue data for joints. These data are extrapolated to other joints. The extrapolation equations are based on a similarity between joints of the same type. The extrapolation is based on empirical evidence. If sufficient data are available, it can imply that the extrapolation is in fact an interpolation. This applies to Larsson's equations for lugs.

The prediction methods for riveted and bolted joints were based on calculated peak stress values. Similar values were supposed to lead to the

same fatigue life. The equations to calculate the peak stress values are based on reasonable arguments. However, the representation of the load transmission in the joint is not covering all aspects which are known to affect the fatigue properties. A more refined procedure was proposed by Jarfall [26, 27], who introduced the stress severity factor (SSF). This factor for riveted joints also accounted for such aspects as hole preparation, residual stress from cold working, interference and fastener flexibility. Empirical data on the influence of these aspects are required to use the SSF. According to Jarfall, life predictions with the SSF are still difficult, but the SSF can be used in design studies. Calculations on load transfer by the fasteners should be made. The SSF then gives comparative indications on the stress severity of the fasteners and design modifications can be considered to reduce the severity of the most critical ones. This approach in essence is designing against fatigue by considering suitable field parameters characterizing the fatigue severity of the joint.

Prediction of crack growth life instead of fatigue life until failure can be an interesting option if fatigue crack growth starts almost immediately. However, it is questionable whether it is useful for bolted and riveted joints. The situation for these joints is complex, particularly for small cracks. Much life is spent by crack initiation and initial growth of small cracks. It implies that the finite element calculation of K-values requires a realistic modeling of a joint to calculate K-values of part through cracks. In view of the complex load transmission in riveted and bolted joints, the FE modeling is a problematic issue. The limitations of predictions are not set by the capacity of computers, neither by available calculation programs, but rather by modeling of the joint details and the mechanisms of fatigue crack initiation and early propagation of small cracks. Consequently, a more efficient solution to obtain fatigue life indications of complex joints should be to collect fatigue test results of similar joints. These results should then be translated to the geometrical conditions of the structure by adopting some suitable field parameter. It could be desirable to carry out some exploratory fatigue tests for this purpose. As emphasized previously, such fatigue test should be carried out on test articles which are representative for the geometry with a load spectrum relevant for the structure.

18.8 Major topics of the present chapter

1. The load transmission in joints is essentially different for lugs, joints with bolts in tension, bolted and riveted joints with shear loaded fasteners and adhesive bonded joints.
2. The fatigue limit of joints can be very low due to severe stress concentrations, fretting corrosion and secondary bending. In spite of a high static strength of a joint, the fatigue limit can be low.
3. Prediction of the fatigue life, fatigue strength and fatigue limit is a complex problem for joints because the crack initiation and initial growth of small cracks cannot easily be compared to a similar behavior in unnotched specimens. This excludes predictions based on basic material fatigue properties. Fatigue properties of joints should be derived from fatigue properties of similar joints for which data are available.
4. The size effect on the fatigue limit of lugs is large. The low fatigue limit of lugs can be significantly improved by plastic hole expansion.
5. Bolts loaded in cyclic tension have a relatively low fatigue strength which can be substantially increased by pre-tensioning.
6. The fatigue strength of symmetric butt joints (riveted or bolted) is superior to the fatigue strength of lap joints. The former joints have no eccentricities, whereas the eccentricity in lap joint causes unfavorable secondary bending and a more complex loading of the fastener on the hole.
7. Hole filling is of great importance to riveted joints. A high rivet squeeze force leads to significant life improvements due to plastic hole expansion and a better clamping between the sheets.
8. Fretting corrosion and local load transmission by fasteners are eliminated in adhesive bonded lap joints. It results in a larger fatigue strength in comparison to similar riveted lap joints. But due attention must be paid to the quality and durability of the bonded joint.

References

1. Schijve, J., *Fatigue of Lugs. Contributions to the Theory of Aircraft Structures*. Nijgh-Wolters Noordhoff Universiy Press (1972), pp. 423–440.
2. Larsson, S.E., *The development of a calculation method for the fatigue strength of lugs and a study of test results for lugs of aluminium alloys*. Fatigue Design Procedures, 4th ICAF Symposium. Pergamon Press (1969), pp. 309–339.

3. Unpublished calculation methods in Technical Handbook No. 3. of Fokker Aircraft Factories, TH3.411.1 (1980).
4. *Fatigue-Endurance Data, Vol. 8*. ESDU Engineering Science Data (1990).
5. Clarke, B.C., *The use of pins with flats to increase the fatigue life of aluminium alloy lugs*. Royal Aircraft Establishment, Farnborough, UK, Tech. Report 66015 (1966).
6. Schijve, J., Broek, D. and Jacobs, F.A., *Fatigue tests on aluminium alloy lugs with special reference to fretting*. Nat. Aerospace Lab. NLR, Report TR M.2103, Amsterdam (1962).
7. Hartman, A. and Jacobs, F.A., *The effect of various fits on the fatigue strength of pin-hole joints*. Nat. Aerospace Lab. NLR, Amsterdam, Report M1946 (1954).
8. Champoux, R.L., *An overview of cold expansion methods*. Fatigue Prevention and Design, J.T. Barney (Ed.), EMAS, Warley (1986), pp. 35–52.
9. Leon, A., *Benefits of split mandrel cold working*. Int. J. Fatigue, Vol. 20 (1998), pp. 1–8.
10. Waters, K.T., *Production methods of cold working joints subjected to fretting for improvement of fatigue strength*. Fatigue of Aircraft Structures. ASTM STP 274 (1959) pp. 99–111.
11. Heywood, R.B., *Designing against Fatigue*. Chapman and Hall, London (1962).
12. Peterson, R.E., *Stress Concentration Factors*. John Wiley & Sons, New York (1974).
13. Shin-ichi Nishida, *Failure Analysis in Engineering Applications*. Butterworth-Heinemann, Oxford (1992).
14. Bonnee, W.J.A., *Investigation of horizontal stabilizer attachment bolts of Astir-gliders*. Nat. Aerospace Lab. NLR, Report TR 80019, Amsterdam (1980).
15. Hertel, H., *Fatigue Strength of Structures*. Springer-Verlag, Berlin (1969) [in German].
16. Shivakumar, K.N. and Newman, J.C., *Stress concentrations for straight-shank and countersunk holes in plates subjected to tension, bending, and pin loading*. NASA-TP-003192 (1992).
17. Niu, M.C., *Airframe Structural Design*. Conmilit Press (1988).
18. Hoffer, K., *Permanent Fasteners for Light-Weight Structures*. Aluminium-Verlag, Düsseldorf (1984).
19. Barrett, R.T., *Fastener Design Manual*. NASA Reference Publication 1228 (1990).
20. Schijve, J., *Some elementary calculations on secondary bending in simple lap joints*. National Aerospace Lab. NLR, Report TR 72036, Amsterdam (1972).
21. Hartman, A. and Schijve, J., *The effects of secondary bending on the fatigue strength of 2024-T3 Alclad riveted joints*. National Aerospace Lab. NLR, Report TR 69116, Amsterdam (1969).
22. Schijve, J., *Multiple-site-damage fatigue of riveted joints*. Proc. Int. Workshop on Structural Integrity of Aging Airplanes. Atlanta Technical Publications (1992), pp. 2–27.
23. Müller, R.P.G., *An experimental and analytical investigation on the fatigue behaviour of fuselage riveted lap joints. The significance of the rivet squeeze force, and a comparison of 2024-T3 and Glare 3*. Doctor thesis, Delft University of Technology (1995).
24. Homan, J. and Jongebreur, A.A., *Calculation method for predicting the fatigue life of riveted joints*. Durability and Structural Integrity of Airframes. Proc. 17th ICAF Symposium, A.F. Blom (Ed.). EMAS (1993) pp. 175–190.
25. Hartman, A., *Fatigue tests on single lap joints in clad 2024-T3 aluminium alloy manufactured by a combination of riveting and adhesive bonding*. National Aerospace Lab. NLR, Report M.2170, Amsterdam (1966).
26. Jarfall, L., *Shear loaded fastener installations*. Int. J. Vehicle Design, Vol. 7 (1986), pp. 337–380.
27. Jarfall, L., *Optimum design of joints: The stress severity factor concept. Aircraft fatigue*. Design, Operational and Economic Aspects, J.Y. Mann and I.S. Milligan (Eds.), Pergamon, Australia (1972), pp. 49–63.

Some general references (see also [12, 14, 19, 20])

28. de Rijck, J.J.M., Homan, J.J., Schijve, J. and Benedictus, R., *The driven rivet head dimensions as an indication of the fatigue performance of aircraft lap joints*. Int. J. Fatigue, Vol. 29 (2007), pp. 2208–2218.
29. de Rijck, J.J.M., *Stress analysis of fatigue cracks in mechanically fastened joints. An analytical and experimental investigation*. Doctor thesis, Delft University of Technology, Delft University Press (2005).
30. Segerfrojd, G., Wang, G.S., Palmberg, B. and Blom, A.F., *Fatigue behaviour of mechanical joints: Critical experiments and statistical analysis*. Fatigue in New and Ageing Aircraft, Proc. 19th ICAF Symposium, R. Cook and P. Poole (Eds.), EMAS, Solihull, UK (1997), pp. 575–598.
31. Toor, P.M. (Ed.), *Structural Integrity of Fasteners*. ASTM STP 1236 (1995).
32. Matek, W., Muhs, D., Wittel, H. and Becker, M., *Roloff/Matek Machinenelementen*, 12th edn. Vieweg & Sohn, Braunschweig (1992) [in German].
33. Bickford, J.H., *An Introduction to the Design and Behaviour of Bolted Joints*, 2nd edn. Marcel Dekker, New York (1990).
34. Jensen, W.J., *Failures of mechanical fasteners*. Failure Analysis and Prevention, Metals Handbook, Vol. 11, (1986), pp. 529–549.
35. Potter, J.M., *Fatigue in mechanically fastened composite and metallic joints*. ASTM STP 927 (1986).